ELSEVIER

Biochimica et Biophysica Acta 1375 (1998) 6–12

BIOCHIMICA ET BIOPHYSICA ACTA
BBA

Effects of the loss of capacity for N-glycosylation on the transport activity and cellular localization of the human reduced folate carrier

So C. Wong, Long Zhang, Susan A. Proefke, Larry H. Matherly *

Experimental and Clinical Therapeutics Program, Barbara Ann Karmanos Cancer Institute and the Department of Pharmacology, School of Medicine, Wayne State University, 110 E. Warren Ave. Detroit, MI 48201, USA

Received 20 March 1998; accepted 22 June 1998

Abstract

The role of N-glycosylation in reduced folate carrier (RFC) transport and membrane targeting was examined in transport-deficient K562 (K500E) cells transfected with human RFC cDNAs. Treatment of cells expressing wild-type RFC with tunicamycin (0–3 μg) resulted in a progressive shift of the ~85 kDa RFC on western blots to 65 kDa. At 3 μg/ml tunicamycin, the nearly complete loss of glycosylated RFC was accompanied by a ~25% decreased rate of methotrexate uptake. A deglycosylated RFC cDNA construct in which asparagine-58 was replaced by glutamine (Gln^{58}-RFC) was expressed in K500E cells as a 65 kDa protein and restored transport capacity for methotrexate and (6*S*)5-formyl tetrahydrofolate. With both wild-type and Gln^{58}-RFC constructs, expression of cDNA-encoded RFC protein far exceeded relative levels of RFC uptake. Wild-type and Gln^{58}-RFCs containing a hemagglutinin (HA) epitope at the carboxyl terminus were similarly functional and, by immunofluorescence staining with rhodamine-conjugated anti-HA antibody, were localized to plasma membranes. Collectively, our results demonstrate that N-glycosylation of human RFC plays no significant role in either transport function or membrane targeting. The discrepancy between the stoichiometries of RFC expression and transport activity for both wild-type RFC and Gln^{58}-RFC implies that identical regulatory controls and/or non-RFC transport components are necessary to completely restore transport function in the transfected cells.

Keywords: Reduced folate carrier; Membrane transport; Glycosylation; Methotrexate; Epitope tagging; Site-directed mutagenesis

1. Introduction

Methotrexate (Mtx) continues to be widely used as an antitumor agent for a variety of malignancies including leukemias, breast cancer, head and neck cancer, lymphomas, and choriocarcinoma [1]. Efficient membrane transport of Mtx by the reduced folate carrier (RFC) is essential for attaining an intracellular level of free drug sufficient to exert maximal inhibition of its intracellular target, dihydrofolate reductase [2,3]. Futhermore, impaired Mtx transport associated with decreased RFC expression or mutations of the RFC protein is a major mechanism of Mtx resistance in cultured cells and patient specimens [4–7].

Abbreviations: Gln^{58}-RFC, RFC containing glutamine substituted for asparagine-58; HA, hemagglutinin; HA-RFC, RFC containing a carboxyl terminal HA epitope; HA/Gln^{58}-RFC, RFC containing glutamine substituted for asparagine-58 and a carboxyl terminal HA epitope; Mtx, methotrexate; RFC, reduced folate carrier; TN, tunicamycin

* Corresponding author. Fax: +1 (313) 832-7294;
E-mail: matherly@kci.wayne.edu

0005-2736/98/$ – see front matter
PII: S0005-2736(98)00118-7

With the isolation and characterization of cDNAs for RFC [8–13], it now becomes feasible to investigate the functional roles of individual amino acids and post-translational modifications that may influence transport activity. The human RFC was originally suggested to differ from the murine transporter in its N-glycosylation [14], and consistent with this notion, a single N-glycosylation consensus site occurs at asparagine-58 in the predicted amino acid sequence for human RFC [10–13]. When expressed in transport-impaired K562 (K500E) cells, the cDNA-encoded protein can be enzymatically deglycosylated [15]. However, the importance of this modification to the intracellular routing and function of the human RFC has not been rigorously confirmed. In this communication, we explore this important question in K500E transfectants expressing human RFC cDNA constructs, through the use of the N-glycosylation inhibitor, tunicamycin (TN; [16]), and site-directed mutagenesis.

2. Materials and methods

2.1. Chemicals

[3′,5′,7-^{3}H]Mtx (20 Ci/mmol) and [3′,5′,7,9-^{3}H](6*S*)5-formyl tetrahydrofolate (20 Ci/mmol) were purchased from Moravek Biochemicals (Brea, CA) and purified prior to use by reverse phase HPLC [17]. Unlabeled Mtx, (6,*R*,*S*)5-formyl tetrahydrofolate, and TN were obtained from the Drug Development Branch, National Cancer Institute, Bethesda, MD.

2.2. Cell culture

The K562 erythroleukemia line was obtained from the American Type Culture Collection (Rockville, MD). Cells were maintained in RPMI 1640 containing 10% heat-inactivated iron-supplemented calf serum (Hydore), 2 mM L-glutamine, 100 U/ml penicillin, and 100 μg/ml streptomycin, in a humidified atmosphere at 37° in the presence of 5% CO_2/95% air. The transport-deficient K500E subline was selected from wild-type K562 cells by cloning in soft agar in the presence of 500 nM Mtx as previously described [15]. The K43-6 subline was derived from K500E cells by transfecting the full-length human RFC cDNA (KS43) constructed in a pCDNA3 expression vector [15]. The characteristics of these cells including levels of RFC expression and transport kinetics were previously described [15].

2.3. Preparation of Gln^{58}-RFC and transfection of K500E cells

Nucleotides 171–174 encoding Asn^{58} (AAC) in the full length KS43 human RFC cDNA [10] were changed to CAG, which encodes for Gln, using a PCR-based site-directed mutagenesis strategy. The mutation primers were 5′-TCCTGGGGCCCGACAAGCAGTTCAC (nucleotide positions 155–179, position 1 is the translation start) and 5′-GCCAGCGAGATGTAGTTGAGCGT (positions 572–550). Following amplification, the 417 bp PCR product was purified, digested with *Apa*I (cleaves within the mutation primer) and *Nco*I (cleaves at position 386–391), and ligated into *Apa*I/*Nco*I-digested KS43 RFC in pBluescript (SK^-). The complete RFC coding region was excised by *Bam*HI and *Xho*I digestions and inserted into a *Bam*HI/*Xho*I-digested pCDNA3 expression vector to generate the Gln^{58}-RFC construct. The Gln^{58}-RFC construct was transfected into the transport-deficient K500E subline using lipofectin (Gibco) and G418 selection as previously described [15]. Positive clones expressing moderate and high levels of Gln^{58}-RFC protein (KEDG1 and KEDG9, respectively) were identified by Western blotting.

2.4. Western analysis of RFC proteins

For the analysis of RFC structures in TN-treated cells, a particulate membrane fraction was prepared by differential centrifugation [14]. For the characterization of the mutagenized RFC constructs stably expressed in K500E cells, the particulate membrane fractions were additionally purified on discontinuous sucrose gradients [14]. Membrane proteins were electrophoresed on 7.5% polyacrylamide gels in the presence of SDS [18] and electroblotted onto PVDF membranes (DuPont). RFC proteins were detected by chemiluminescence (Pierce, Rockford, IL) using a protein A-purified RFC specific peptide antibody (RFC/ps, [19]), or antibody prepared in rabbits to a

glutathione *S*-transferase (GST)-RFC fusion protein, expressed in *Escherichia coli* and purified by glutathione-Sepharose 4B chromatography (S.C. Wong, L. Zhang, S.A. Proefke, T.L. Radewan, A. Bhushan, and L.H. Matherly, manuscript submitted). Light emission was recorded on X-ray film with various exposure times to avoid overexposure. Signals were analyzed using a computing densitometer and ImageQuant software (Molecular Dynamics, Sunnyvale, CA).

2.5. Preparation of epitope-tagged RFC and immunolocalization of HA-RFC proteins

A hemagglutinin (HA) peptide epitope (YPYDVPDYASL, [20]) was fused to the human RFC carboxyl terminus by PCR-based site-directed mutagenesis. The downstream primer used for introducing the HA epitope was 5′-GGTACCTCGAGTCAGAGGCTAGCGTAATCCGGAACATCGTATGGGTACTGAACACCGTCGCTTGGAA. A *Xho*I restriction site was included for subcloning. The upstream RFC specific primer used was 5′-CCTGGTCTTCGGGGTCAACA (positions 1191–1211 in KS43 RFC cDNA). The PCR product was purified, digested with *Xho*I and *Eco*RI (positions 1603–1608), and ligated into *Eco*RI/*Xho*I-digested KS43 in pCDNA3 [10] to generate the HA-RFC plasmid construct. A carboxyl HA-tagged Gln^{58}-RFC construct (HA/Gln^{58}-RFC) was prepared in an identical fashion using *Eco*RI/*Xho*I-digested Gln^{58}-RFC for ligation. Both the HA-RFC and HA/Gln^{58}-RFC constructs in pCDNA3 were transfected into K500E cells, as described above. Based on the level of RFC expression on Western blots, HA8 (expresses HA-RFC) and HA-DG32 (expresses HA/Gln^{58}-RFC) sublines were selected for further studies.

A commercially available rhodamine-conjugated anti-HA monoclonal antibody (12CA5; Boehringer Mannheim) was used to localize HA-tagged RFC proteins by immunofluorescence. HA8, HA-DG32 and K500E cells ($5–10\times10^6$) were washed in ice-cold PBS and fixed in 2 ml of 3.3% paraformaldehyde in PBS on ice for 30 min. Cells were washed twice in PBS and permeabilized in 2 ml of 0.1% Triton X-100 in PBS for 5 min at 4°C. Permeabilized cells were washed (2×) in PBS and samples (2.5×10^6 cells) incubated in 1 ml of PBS containing 1% bovine serum albumin and 5 μg of rhodamine-conjugated 12CA5 antibody for 1 h at 4°C. Fluorescent-labeled cells were washed (2×) in PBS and resuspended at a density of 50 000 cells/ml; 200 μl of cells were cytocentrifuged onto microscope slides, mounted with one drop of 'SlowFade' antifade reagent (Molecular Probes) and sealed with cover slips. Slides were observed under a Zeiss laser scanning microscope 310 at 543 nm and 630× magnification.

2.6. Membrane transport measurements

Initial uptake rates for [^{3}H]Mtx and [^{3}H](6*S*) 5-formyl tetrahydrofolate were determined over 180 s as previously described [14], using $0.5–1\times10^7$ cells/ml. The levels of intracellular radioactivity were expressed as pmol/mg protein, calculated from direct measurements of radioactivity and protein contents of the cell homogenates. Protein assays were by the method of Lowry et al. [21]. Kinetic constants (K_t and V_{max} values) were calculated from Lineweaver–Burk plots from initial uptake rates over a range of substrate concentrations.

3. Results and discussion

Oligosaccharide side chains of membrane proteins have been shown in many instances to be important for proper function, membrane targeting and transmembrane signaling [22]. TN, an inhibitor of core oligosaccharide addition to asparagine residues of nascent glycoproteins [16], was initially used to assess the roles of N-linked glycosylation in RFC-mediated Mtx transport and membrane targeting. K43-6 transfectants, expressing increased levels of human RFC [15], were cultured with 0, 1, 2 and 3 μg/ml of TN over 16 days (10–11 generations), after which cells were harvested for Western analysis of RFC protein in particulate membrane and soluble fractions, and assays of [^{3}H]Mtx uptake. A dose-dependent inhibition of N-glycosylation was clearly evident with increasing TN, as indicated by the progressive shift of the broadly-migrating RFC band (centered at ~85 kDa for the gel in Fig. 1, left panel) in the particulate fraction to a condensed band at 65 kDa. This is the size predicted from the RFC coding sequence [10]. At 3 μg/ml TN, almost all membrane

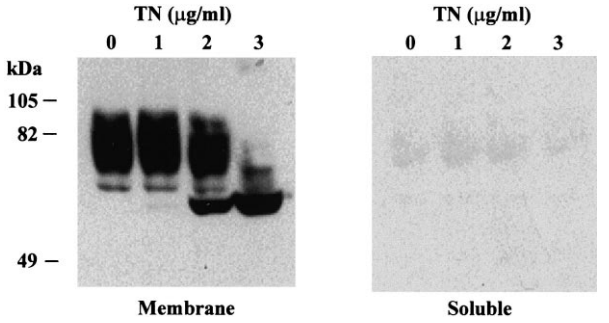

Fig. 1. Inhibition of RFC glycosylation by TN. Particulate membrane (30 μg) and soluble (100 μg) proteins from K43-6 cells, cultured in the presence of TN (0, 1, 2 or 3 μg/ml) for 16 days, were fractionated on a 7.5% gel in the presence of SDS and electroblotted onto a PVDF membrane. Detection was with an anti-RFC peptide antibody (RFC/ps; [19]) and an enhanced chemiluminescence kit. Migrations of the molecular weight markers are indicated.

RFC protein was deglycosylated (Fig. 1, left panel). Immunoreactive RFCs were virtually undetectable in the soluble fraction in TN-treated cells, even when 3-fold more protein was analyzed, suggesting that there was no effect on membrane localization (Fig. 1, right panel). While treatments of K43-6 cells with 1 or 2 μg/ml TN had no effect on initial uptake of [^{3}H]Mtx (at 0.5 μM) over 180 s, the nearly complete loss of N-glycosylated RFC at 3 μg/ml TN was accompanied by a ~25% decreased Mtx uptake rate (data not shown).

Although TN treatments had negligible effects on cell proliferation, secondary metabolic effects including inhibition of protein synthesis [16] or effects on non-RFC glycosylation could compromise analysis of changes in Mtx transport in TN-treated cells. To obviate this concern, we used site-directed mutagenesis to replace Asn^{58} with Gln, thereby eliminating the N-glycosylation consensus site in the resulting Gln^{58}-RFC construct. In order to assess the plasma membrane localization of wild-type and Gln^{58}-RFCs, additional RFC constructs were prepared in which an HA peptide epitope was inserted into the RFC carboxyl terminus. HA-RFC, HA/Gln^{58}-RFC, and Gln^{58}-RFC constructs were all transfected into transport-deficient K500E cells and stable clones (HA8, HA-DG32, and KEDG1 and KEDG9, respectively; Table 1) selected for further analysis.

Initial rates of [^{3}H]Mtx uptake were measured for the transfected lines and compared to wild-type K562, untransfected K500E cells, and the K43-6 transfectants expressing wild-type RFC [15]. For all the RFC transfectants, Mtx uptake equaled (KEDG1) or slightly exceeded (K43-6, KEDG9, HA8, HA-DG32) the level for wild-type K562 cells, and exceeded that in K500E cells by 6.6–24.9-fold (Table 1). There were no differences in either V_{max} or K_t values for Mtx between the K500E transfectants expressing glycosylated (K43-6) and Gln^{58}-(KEDG9) RFCs, or carboxyl HA-RFC (HA8) (Table 2). Likewise, relative uptake of [^{3}H](6*S*)5-formyl tetrahydrofolate (at 0.5 μM) varied only slightly (less than 2-fold) between wild-type K562, K43-6, KEDG9, and HA8 cells (not shown).

On Western blots of purified plasma membrane proteins, Gln^{58}- and HA/Gln^{58}-RFCs both appeared as 65 kDa bands (KEDG1 and 9, and HA-DG32,

Table 1
Mtx uptake rates and relative RFC expression in K562 sublines[a]

Cell line	RFC construct[b]	Uptake[c] (pmol/mg/min)	Relative uptake[d]	Relative RFC expression[e]
K500E	–	0.15 ± 0.03	0.18	0.03
K562	–	0.85 ± 0.07	1.00	1.00
K43-6	KS43	2.99 ± 0.36	3.52	20.00
KEDG1	Gln^{58}-RFC	1.00 ± 0.07	1.18	4.00
KEDG9	Gln^{58}-RFC	2.44 ± 0.11	2.87	39.00
HA8	HA-RFC	3.62 ± 0.10	4.26	144.65
HA-DG32	HA/Gln^{58}-RFC	3.81 ± 0.27	4.48	41.60

[a]Uptake of 0.5 μM [^{3}H]Mtx was measured as described in Section 2.
[b]The RFC constructs are KS43 (wild-type RFC), Gln^{58}-RFC (RFC containing Gln for Asn^{58}); HA-RFC (RFC containing a carboxyl terminal HA epitope), and HA/Gln^{58}-RFC (RFC containing glutamine for asparagine-58 and a carboxyl terminal HA epitope).
[c]Uptake values are reported as mean values ± S.E.M from two to three experiments.
[d]Relative Mtx uptake compared to wild-type K562 cells.
[e]Relative RFC expression was normalized to RFC signal measured by densitometry per μg membrane protein.

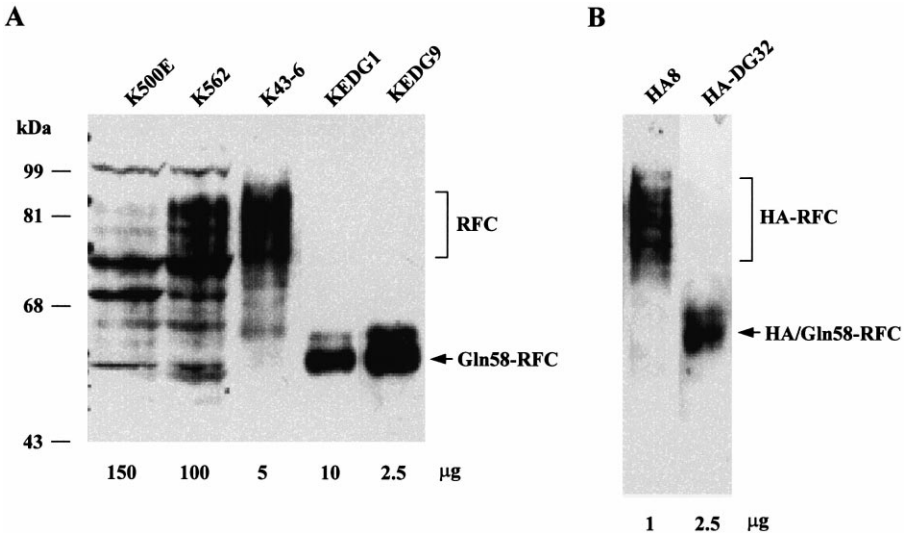

Fig. 2. Western blotting of glycosylation-defective mutant RFCs and epitope-tagged RFCs in transfected K500E cells. Sucrose gradient-purified membrane proteins from Gln^{58}- and HA-RFC transfectants (KEDG1, KEDG9, HA8 and HA-DG32), wild-type RFC transfectants (K43-6), and untransfected K500E and wild-type K562 cells were fractionated on a 7.5% gel in the presence of SDS and electroblotted onto a PVDF membrane. Detection was with anti-GST-RFC antibody and an enhanced chemiluminescence kit. The amounts of membrane protein analyzed for each line and the molecular standards are noted. A and B are from the same Western blot exposed to X-ray film for different times. The bands representing the full-size RFC, Gln^{58}-RFC, HA-RFC, and HA/Gln^{58}-RFC are noted.

respectively), clearly distinguishable from the glycosylated RFC forms in K43-6 and HA8 cells (Fig. 2). By immunofluorescence staining with rhodamine-conjugated 12CA5 antibody, both HA8 and HA-DG32 cells exhibited prominent rhodamine staining localized to the cell membranes (Fig. 3D and F, respectively), indicating that the lack of N-glycosylation has no effect on RFC membrane targeting. Although low level staining was also detected in K500E cells, there was no specific staining of the plasma membrane surface (Fig. 3B).

We previously reported [15] that K43-6 cells exhibit a disparate level of RFC protein (~20-fold increased over wild-type cells in Fig. 2) to restored Mtx transport, and analogous results were obtained for the Gln^{58}- and HA-RFC constructs (Fig. 2 and Table 1). Levels of maximal Mtx uptake were nearly identical in the transfected lines (~3–4-fold over wild-type) regardless of levels of RFC expression. When Mtx uptake was normalized to RFC expression for the transfectants, relative levels ranged from 0.029 to 0.30 and clearly showed that neither the Gln^{58}- nor HA-modifications of RFC appreciably altered transport function compared to wild-type RFC.

Hence, our results demonstrate that inhibition of human RFC N-glycosylation by treatment with TN, or elimination of the RFC N-glycosylation consensus site by site-directed mutagenesis has little or no significant effect on either transport function or membrane targeting for the human RFC. In spite of high levels of surface expression, for both glycosylated and non-glycosylated carriers, the low efficiency of the restored transport approximates only 3–30% of that expected from the levels of immunoreactive RFCs. Indeed, our results add to the growing list of discordant properties between transfected and endogenous RFCs, including specificities for transport

Table 2
Kinetic constants for Mtx influx[a]

Cell line	V^b_{max} (pmol/mg/min)	K^b_t (μM)
K562	5.93 ± 1.05	3.07 ± 0.40
K43-6	10.74 ± 0.38	1.65 ± 0.20
KEDG9	9.04 ± 1.26	1.49 ± 0.22
HA8	10.86 ± 1.91	1.16 ± 0.23

[a]Kinetic constants for Mtx transport were calculated by Lineweaver–Burk analysis.
[b] V_{max} and K_t values are reported as mean values ± S.E.M. (n=2).

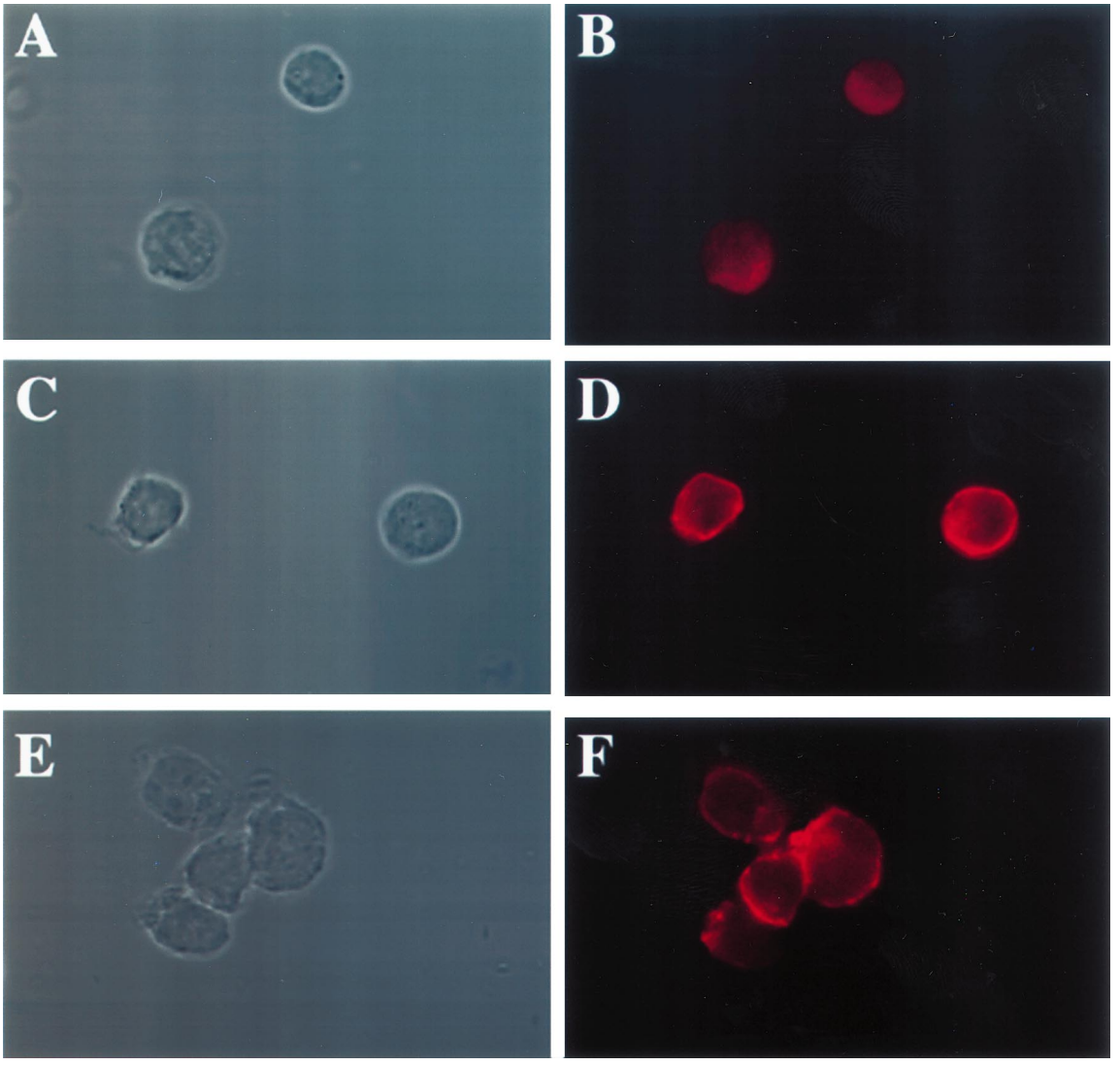

Fig. 3. Immunofluorescence microscopy of HA8 and HA-DG32 cells. HA8 (C,D) and HA-DG32 (E,F) cells were processed for immunofluorescence staining with rhodamine-conjugated 12CA5 monoclonal antibody as described in Section 2. Untransfected K500E cells (A,B) were used as negative control.

substrates [10,23,24], pH optima [23–25], and bidirectional transport fluxes for Mtx [26]. Collectively, these differences suggest a complex modulation of transporter function which distinguishes endogenously-expressed from transfected RFCs, and involving as-yet uncharacterized regulatory controls and/or requirements for non-RFC transport components [15].

Acknowledgements

This research was supported by NIH Grant CA53535. The excellent technical assistance of Ms. Teah Radewan with some of the experiments is acknowledged.

References

[1] J. Jolivet, K.H. Cowan, G.A. Curt, N.J. Clendeninn, B.A. Chabner, The pharmacology and clinical use of methotrexate, New Engl. J. Med. 309 (1983) 1094–1104.
[2] I.D. Goldman, L.H. Matherly, The cellular pharmacology of methotrexate, Pharmacol. Ther. 28 (1985) 77–102.
[3] F.M. Sirotnak, Obligate genetic expression in tumor cells of a fetal membrane properties mediating 'folate' transport:

biological significance and implications for improved therapy for human cancer, Cancer Res. 45 (1985) 3992–4000.
[4] J.D. Schuetz, L.H. Matherly, E.H. Westin, I.D. Goldman, Evidence for a functional defect in the translocation of the methotrexate transport carrier in a methotrexate-resistant murine L1210 leukemia cell line, J. Biol. Chem. 263 (1988) 9840–9847.
[5] K.E. Brigle, M.J. Spinella, E.E. Sierra, I.D. Goldman, Characterization of a mutation in the reduced folate carrier in a transport defective L1210 murine leukemia cell line, J. Biol. Chem. 270 (1995) 22974–22979.
[6] M. Gong, J. Yess, T. Connolly, S.P. Ivy, T. Ohnuma, K.H. Cowan, J.A. Moscow, Molecular mechanism of antifolate transport deficiency in a methotrexate resistant MOLT-3 human leukemia cell line, Blood 89 (1997) 2494–2499.
[7] R. Gorlick, E. Goker, T. Trippett, P. Steinherz, Y. Dlisseyeff, M. Mazumdar, W.F. Flintoff, J.R. Bertino, Defective transport is a common mechanism of acquired methotrexate resistance in acute lymphocytic leukemia and is associated with decreased reduced folate carrier expression, Blood 89 (1997) 1013–1018.
[8] K.H. Dixon, B.C. Lanpher, J. Chiu, K. Kelley, K.H. Cowan, Novel cDNA restores reduced folate carrier activity and methotrexate sensitivity to transport deficient cells, J. Biol. Chem. 269 (1994) 17–20.
[9] F.M.R. Williams, R.C. Murray, T.M. Underhill, W.F. Flintoff, Isolation of a hamster cDNA clone coding for a function involved in methotrexate uptake, J. Biol. Chem. 269 (1994) 5810–5816.
[10] S.C. Wong, S.A. Proefke, A. Bhushan, L.H. Matherly, Isolation of human cDNAs that restore methotrexate sensitivity and reduced folate carrier activity in methotrexate transport-defective Chinese hamster ovary cells, J. Biol. Chem. 270 (1995) 17468–17475.
[11] J.A. Moscow, M. Gong, R. He, M.K. Sgagias, K.H. Dixon, S.L. Anzick, P.S. Meltzer, K.H. Cowan, Isolation of a gene encoding a human reduced folate carrier (RFC1) and analysis of its expression in transport-deficient, methotrexate-resistant human breast cancer cells, Cancer Res. 55 (1995) 3790–3794.
[12] F.M.R. Williams, W.F. Flintoff, Isolation of a human cDNA that complements a mutant hamster cells defective in methotrexate transport, J. Biol. Chem. 270 (1995) 2987–2992.
[13] P.D. Prasad, S. Ramamoorthy, F.H. Leibach, V. Ganapathy, Molecular cloning of the human placental folate transporter, Biochem. Biophys. Res. Commun. 206 (1995) 681–687.
[14] L.H. Matherly, C.A. Czajkowski, S.M. Angeles, Identification of a highly glycosylated methotrexate membrane carrier in K562 erythroleukemia cells up-regulated for tetrahydrofolate cofactor and methotrexate transport, Cancer Res. 51 (1991) 3420–3426.
[15] S.C. Wong, R. McQuade, S.A. Proefke, A. Bhushan, L.H. Matherly, Human K562 transfectants expressing high levels of reduced folate carrier but exhibiting low transport activity, Biochem. Pharmacol. 53 (1997) 199–206.
[16] A.D. Elbein, Inhibitors of the biosynthesis and processing of N-linked oligosaccharide chains, Annu. Rev. Biochem. 56 (1987) 497–534.
[17] D.W. Fry, J.C. Yalowich, I.D. Goldman, Rapid formation of polyglutamyl derivatives of methotrexate and their association with dihydrofolate reductase as assessed by high pressure liquid chromatography in the Ehrlich ascites tumor cells, J. Biol. Chem. 257 (1982) 1890–1896.
[18] U.K. Laemmli, Cleavage of structural protein during bacteriophage T4, Nature 227 (1970) 680–685.
[19] S.C. Wong, L. Zhang, S.A. Proefke, B. Hukku, L.H. Matherly, Gene amplification and increased expression of the reduced folate carrier in transport elevated K562 cells, Biochem. Pharmacol. 55 (1998) 1135–1138.
[20] I.A. Wilson, H.L. Niman, R.A. Houghten, A.R. Cherenson, M.L. Connolly, R.A. Lemer, The structure of an antigenic determinant in a protein, Cell 37 (1984) 767–778.
[21] O.H. Lowry, N.J. Rosebrough, A.L. Farr, R.J. Randall, Protein measurement with the Folin phenol reagent, J. Biol. Chem. 193 (1951) 265–275.
[22] C.G. Gahmberg, M. Tolvanen, Why mammalian cell surface protein are glycoproteins, Trends Biochem. Sci. 21 (1996) 308–311.
[23] J.H. Chiao, K. Roy, B. Tolner, C.H. Yang, F.M. Sirotnak, RFC-1 gene expression regulates folate absorption in the mouse small intestine, J. Biol. Chem. 272 (1997) 11165–11170.
[24] C.K. Kuman, T.T. Nguyen, F.B. Gonzales, H.M. Said, Comparison of intestinal folate carrier expressed in IEC-6 cells and Xenopus oocytes, Am. J. Physiol. 274 (1998) C289–C294.
[25] T.T. Nguyen, D.L. Dyer, D.D. Dunning, S.A. Rubin, K.E. Grant, H.M. Said, Human intestinal folate transport: cloning, expression and distribution of the complementary RNA, Gastroenterology 112 (1997) 783–791.
[26] R. Zhao, R. Seither, K.E. Brigle, I.G. Sharina, P.J. Wang, I.D. Goldman, Impact of overexpression of the reduced folate carrier (RFC1), an anion exchanger, on concentrative transport in murine L1210 leukemia cells, J. Biol. Chem. 272 (1997) 21207–21212.